Escaping Near-relativistic Electron Beams from the Solar Corona

D. K. Haggerty[1], E. C. Roelof[1] , and G. M. Simnett[2]

[1]*Johns Hopkins University/Applied Physics Laboratory, Laurel, MD 20723, USA*
[2]*School of Physics and Astronomy, University of Birmingham, Birmingham, B152TT, UK*

ABSTRACT

The solar corona is a prodigious accelerator of energetic ions, and electrons and the angular distribution, composition, and spectra of energetic particles observed near Earth gives information on the acceleration mechanisms. A particular class of energetic particle observations found useful in understanding the solar acceleration are the near-relativistic impulsive beam-like electron events. During five years of operation The Advanced Composition Explorer (ACE) has made measurements of well over 400 electron events. Approximately 25% of these electron events are impulsive beam-like events and are released onto interplanetary field lines predominantly from western solar longitudes. We extend our initial ~3 year study during the rise to solar maximum (Haggerty & Roelof, 2002; Simnett, Roelof, and Haggerty, 2002) to a five year statistical analysis of these beam-like energetic electron events in relationship to optical flares, microwave emission, soft X-ray emission, metric and decametric type-III radio bursts, and coronal mass ejections.

INTRODUCTION

Large solar flares and their coronal mass ejections (CMEs) are associated with the acceleration and release of large fluences of energetic ions and electrons that are observed in the inner heliosphere in two distinct groups; the Energetic Storm Particle (ESP) event and the Solar Energetic Particle (SEP) event. The ESP events are observed in direct association with the interplanetary shock, driven by the propagating CME. Although the main constituent in ESP events is energetic ions, an intensity increase of energetic electrons is also observed in the larger events. The mechanism for the acceleration and release of the energetic particles has remained elusive. Simnett, (1974) showed that the onsets of fully relativistic electron bursts observed near Earth were delayed relative to solar flare EM emissions by > 10 minutes. Cliver et al., 1982 and Kahler, 1994 showed that the onsets for energetic protons > 10 MeV and the onsets for ground level events (GLE) were also related to CME driven shocks in the high corona with a typical release altitude of > 2 R_o. Recent studies have shown that the near-relativistic beam-like electron events observed at the L1 Lagrangian orbit are released onto open field lines ~10 minutes after metric and decametric type III radio bursts (Krucker et al., 1999; Haggerty and Roelof, 2002) as well as microwave, optical flare, and soft X-ray (SXR) emission (Haggerty and Roelof, 2002). These scatter-free electron events were found to be directly related to CMEs with the intensity and spectral hardness of the electron events correlated with the speed of the CME (Simnett et al., 2002). For this study we have examined five years of ACE/EPAM (Electron, Proton, and Alpha monitor) near-relativistic electron observations, microwave, metric, and decametric radio emission, Hα optical flare emission, and SOHO/LASCO CME images. We report on timing delays between the injection of the SEP electron beams and various EM emissions. We also report on the correlations between the CMEs and the injection of the electron events.

EVENT CRITERIA

The EPAM instrument (Gold et al., 1998) measures near-relativistic electrons (38<E<315) keV in three different detector telescopes at 30°, 60°, and 150° from the spacecraft spin axis. These detectors sample much of the 4π solid angle at a resolution of up to 1.5 seconds/sector and supply the required angular distributions for the

study. From the launch of ACE (Aug 25, 1997) through Mar 31, 2002 EPAM observed 406 near-relativistic electron events. A wide variety of intensity variations, angular distributions, and spectral evolution are observed in the events, so a precise method of selecting only well connected, scatter-free, beam-like electron events needs to be established. The method we have employed consists of three clearly defined observations:

1. A scatter-free onset. The observation of velocity dispersion is required, this also demands that the event is observed in at least two channels and the minimum energy of the electron beam is E>53 keV.
2. A field aligned angular distribution. The electron pitch angle distribution (PAD) must be 'beam-like' along the IMF.
3. An unambiguous onset time. The event onset needs to have a large enough signal to noise ratio (SNR) that the onset time can be firmly established.

Based on these criteria 113 near-relativistic, scatter-free, beam-like electron events (28% of 406) were selected for this study. Two different methods for determining the precise electron event injection time at the Sun have been reported. Krucker et al. (1999) identified injection times by plotting channel onset times versus inverse channel velocity. A straight-line fit to the points yields both the path length traveled and the release time at the sun. The method used for this study, Haggerty and Roelof (2002), uses the extremely collimated electron PADs from the highest energy channel in which they were measured. The injection time is shifted back from the onset time by a transit time of 1.2 AU divided by the velocity in that highest channel. A comparison of the two methods gives an approximately normal distribution with zero mean and a standard deviation of 2.5 minutes (S. Krucker 2002, private communication). We therefore conclude that the method employed by Krucker et al. (1999) and the method used in this study (Haggerty and Roelof, 2002) yield effectively the same results.

The CME coronagraph images were obtained from the Large Angle and Spectrometric Coronagraph Experiment (LASCO) C2 on the Solar and Heliospheric Observatory (SOHO). CME launch times were determined via the standard technique of mapping the height-time profiles back to 1 $R_{O,}$ while the speed to the CME is directly determined from the slope of the height-time profile. See Simnett et al. (2002) for a thorough discussion on the CME identification and analysis. Owing to several factors LASCO was not observing during 30 of the 113 events. In the remaining 83 electron events, 70 (84%) well correlated CMEs were observed.

The decametric radio burst observations are made using high resolution (16 second) WIND/WAVES (Bougeret et al. 1995) data. The timing of the type III radio bursts observed at 14 MHz (~ $2R_O$ based on the density model of Leblanc et al., 1998) was obtained by taking a frequency cut of the WAVES channel associated with 14 MHz emission. The timing of the peak of the 14 MHz frequency cut was used as the timing of the decametric type III emission. A one-to-one correlation was obtained for all 111 of the electron events for which WIND/WAVES data were available. The timing of the decametric type III emission (observed near 1 AU) and all of the EM emissions used in this study are taken back to the Sun by 500 seconds so we may refer to them as an emission time, not just an observed time.

The time of the remaining EM emissions used in this study, microwave and metric radio bursts, Hα optical flares and SXR emission were obtained from the NOAA Solar Geophysical data (SGD). For some of the electron events, multiple metric type IIIs, Hα flares, or SXR events fell within a ±1 hour interval of possible association. To ensure we were not biasing the selection of EM events, we included all events within the interval. There were 20 electron events with no reported metric type III emission (±1 hour of electron injection) in the SGD. For the remaining 93 events, a total of 174 metric type III radio bursts fell within the timing intervals and have been included in the statistical analysis presented in this study. There were 26 electron events with no SXR emission reported while 7 electron events had multiple possible SXR associations. The total number of 87 (77%) of the beam like electron events have associated SXR emission. There were 39 electron events with no reported Hα optical flare reported in the SGD. Of the remaining 74 events, 26 had at least two possible Hα observations within the prescribed interval. Therefore the total number of Hα observations presented in this study is 116 that are correlated with 79 near-relativistic electron events. There were 75 electron events with no reported microwave bursts (> 8800 MHz) in the SGD. Of the remaining 38 (33%) electron events, 4 had multiple microwave bursts reported yielding a total of 43 microwave bursts used in this study.

WELL CONNECTED ELECTRON EVENTS

While the event selection criteria results in a list of electron events that propagate scatter-free, that are field-aligned, and that are clean enough to use in a statistical timing study, they do not demand that the selected events be well connected to western longitudes. While we do not argue that these electron events are accelerated at the flare site, we will use the longitude of the Hα flares to estimate the approximate longitude of the electron injection. The left panel of Figure 1 shows that the longitude of the electron-event-correlated Hα flares had a median longitude of

44°. Note that the majority of Eastern flares shown in Figure 1 have at least one Western flare that was associated with the same electron event and are therefore probably not associated with the electrons that arrive at 1 AU. On the ordinate of the left panel of Figure 1 is the time delay between the start time of the optical flare and the injection of the near-relativistic electrons. We find no clear trend in these observations that would indicate that the electron injection delay is related to the longitude of the associated event.

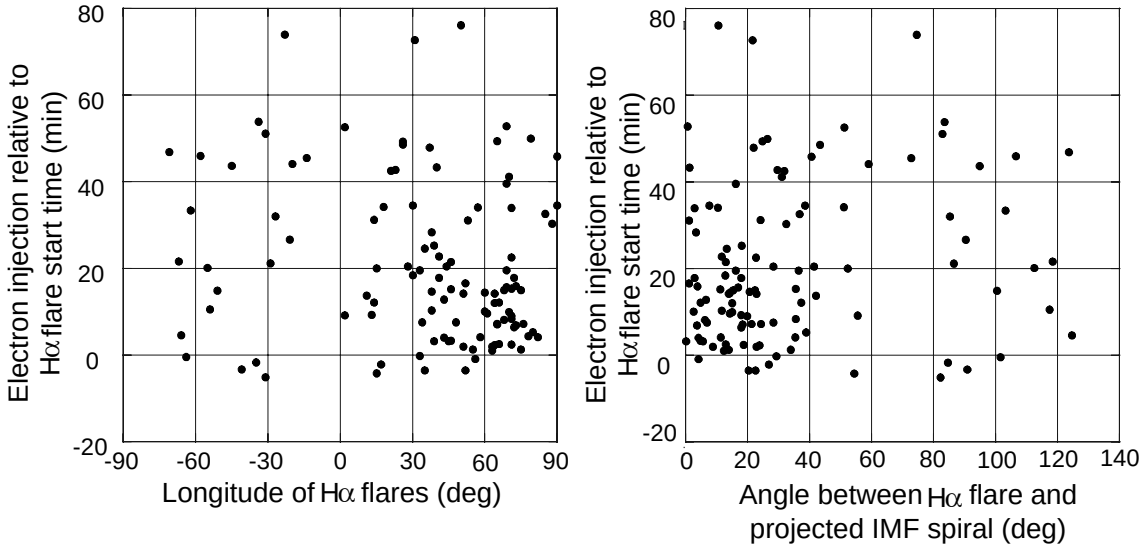

Fig. 1. Left panel. Longitude of Hα flares verses the time delay between start time of the flare and the electron injection. Right panel. Angle between the longitude of the Hα flare and the projected longitude of IMF connection based on the solar wind speed at the time of the electron onset verses the time delay between start time of the flare and the electron injection.

With the magnetic-field lines frozen into the expanding plasma at a source surface in the corona, one may estimate the actual longitude of IMF connection based on the local plasma speed at the time of the electron onsets. The right panel in Figure 1 shows the difference between the angle of the Hα longitude and the projected IMF spiral angle versus the time delay between the optical flare start time and the electron event injection. Although this gives another estimate of how well connected the optical flare site is to the L1 orbit, it does not seem to order the delays. Nor is any clear pattern revealed through this combination of observations that would indicate acceleration and release of electrons due to a source propagating along the solar surface.

LOW CORONAL ELECTROMAGNETIC EMISSION

The traditional view of HXR emission from the low corona consists of a beam of non-thermal electrons being driven down the coronal field lines into the chromosphere where thick target bremstralung results in the emission of the HXR. Timing between the escaping population of energetic electrons and these low coronal emissions can indicate if the escaping population is accelerated through the same process. Microwave emission and HXR emissions are well correlated, and the emission time between them is known to differ by less than a few seconds. We therefore take the microwave emission as a proxy of the HXR event. Figure 2 shows the distribution of timing delays between the injection of the escaping near-relativistic electron beams and the microwave emission. While a few of the electron events in our list are associated with the start time of the microwave events (t=0 indicates the start time of the microwave radio emission), the median delay of the injection of the escaping population is 14 minutes (average 13 minutes).

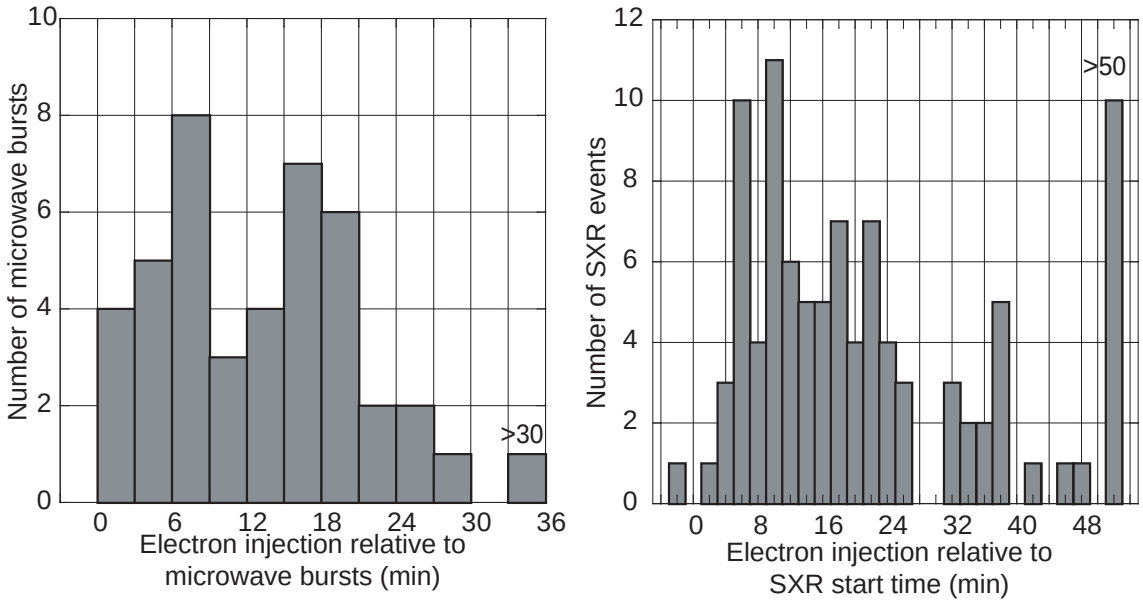

Fig. 2. Left panel. Distribution of delay times at the Sun between the injection of the escaping near-relativistic electron beams and the emission of the microwave radio bursts. Right panel. Distribution of delay times at the Sun between the escaping population and the SXR emission.

The right panel of Figure 2 shows the distribution of delays between the injection of the escaping population of near-relativistic electrons and the start time of the SXR event. The last histogram in the right panel of Figure 2 at t=52, indicates the integral of the distribution that extends beyond t>50 minutes. The median delay between the escaping population and the SXR start time is 17 minutes. Comparisons to both the HXR (microwave) start time and the SXR start time show that the injection of the escaping near-relativistic electrons is delayed by ~10 minutes relative to the start of the solar flare process.

TWO DISTINCT POPULATIONS OF ESCAPING ELECTRONS

Type III radio bursts are known to be produced by plasma-wave interactions from electron beams escaping into the high corona and interplanetary space. The energy of the electrons within the escaping beam are known to be non-thermal and contain a spectrum of electron energies. The speed at which the type III exciter front propagates corresponds to an electron energy of a few keV (Haggerty, Roelof, and Kaiser, 2001; Haggerty and Roelof, 2002). We have shown that the injection of the escaping population of near-relativistic electrons is delayed with respect to optical flares observed in Hα as well as low coronal HXR and SXR emission. We now show that a similar delay exists between the injection of the escaping energetic electrons and the type III producing lower energy electrons. Figure 3 shows the distribution of delays with respect to the metric type III (left) and the decametric type III radio bursts (right). In both figures t=0 is the start time of the type III emission and the histograms detail the distribution of the energetic electron injection delays. The last histogram at t=50 in the left panel of Fig. 3 represents the integral of the distribution that extends beyond t>50 minutes. The median delay between the start time of the metric type III radio burst and the injection of the near-relativistic electrons is ~13 minutes while the median delay between the start time of the decametric type III radio burst and the injection of the high energy electrons is ~8 minutes. These histograms give direct evidence that the injection of the near-relativistic electrons that are observed at 1 AU are significantly delayed with respect to the type III radio bursts. No evidence is observed in either of the histograms that near-relativistic (E>53 keV) electrons are part of the electron population that produce the type III emission, at least to a significant SNR at EPAM (see Haggerty and Roelof, 2002 for an analysis of the SNR and quality of the observed onsets).

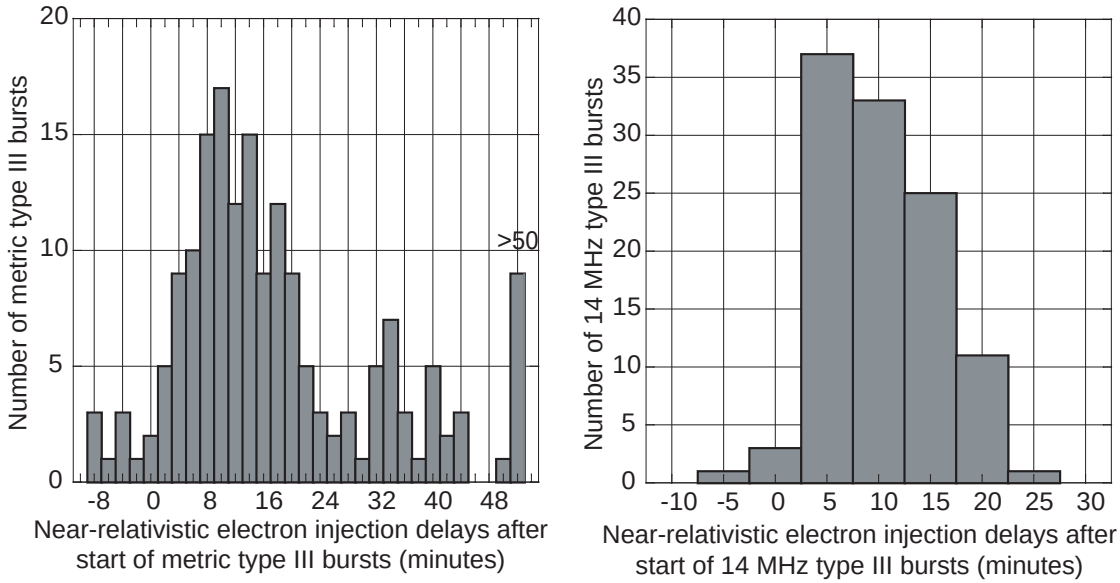

Fig. 3. The delay between the injection of the near-relativistic electron beams and the start time of the metric type III radio bursts (left) and the peak time of the decametric type III radio bursts (right). The time (t=0) in each panel indicates the start time/peak time of the metric/decametric type III radio burst.

RELATIONSHIP BETWEEN ELECTRON INJECTIONS AND CMEs

Simnett et al. (2002) showed evidence that the injection of the near-relativistic electron beams is delayed with respect to the launch of the CME, that the height of the CME at the time of electron injection is a few R_o, and that the speed of the CME is related to both the intensity and the spectral hardness of the electron event. The event list used by Simnett et al. (2002) contained 79 of the electron events included in this study. We will now show that the evidence presented by Simnett et al. (2002) is supported by our extended list. The left panel of Fig 4 shows the height of the CME at the time of electron injection and similar to other figures, the right-most bin represents the total number of CME heights > 5 R_o. The median height of the CME when the energetic electron are injected is 2.4 R_O, in agreement with Simnett et al. (2002). The right panel shows that the delay between the injection of the electrons and the launch of the CME is inversely proportional to the velocity of the CME. In other words fast CMEs are associated with shorter delay times while slow CMEs are associated with longer delay times.

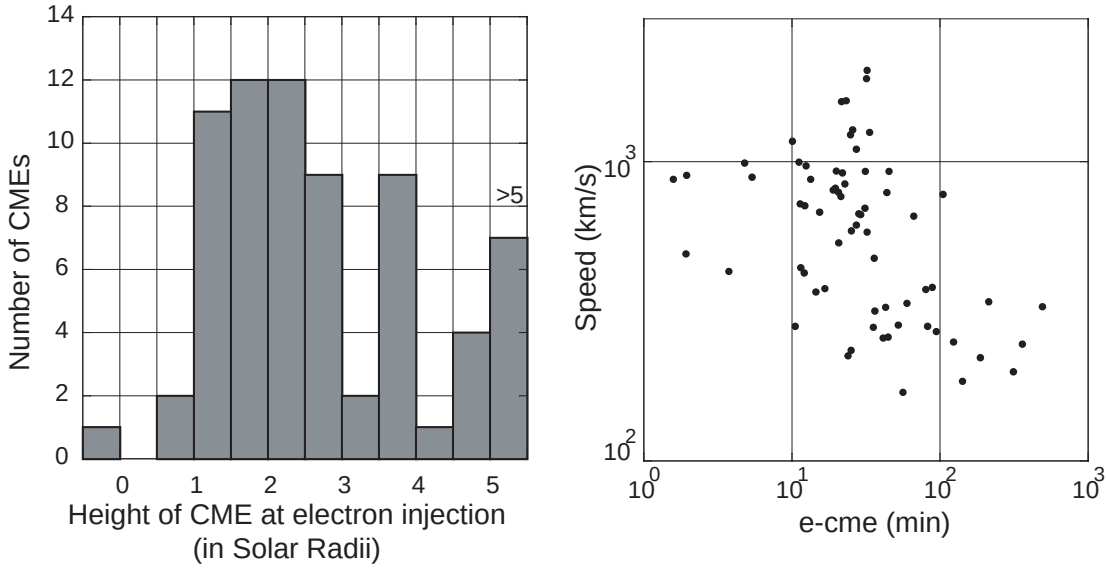

Fig. 4. Left panel. Height of the CME at the time of near-relativistic electron injection. Right panel. Delay between the injection of the energetic electrons and the launch of the CME on the abscissa with the speed of the CME on the ordinate.

DISCUSSION AND CONCLUSIONS

It has been known for years that the high energy ions (Kahler, 1994) and relativistic electrons (Simnett, 1974; Cliver et al. 1982) are accelerated and released into the interplanetary medium with a delay time with respect to related EM emissions in large solar flares. It was suggested that the ions, and possibly electrons, are accelerated by a CME driven shock and that the delay is due to the shock propagating to open field lines where they have access to monitoring instruments. Only recently has it been clearly shown that the near-relativistic electrons show a similar delay (Krucker et al. 1999; Haggerty and Roelof, 2002) and that the delay is inversely correlated with the speed of the CME, that the height of the CME at the time of the injection of the electrons is a few R_O, and that the intensity and spectral harness of the near-relativistic electron events is directly related to the speed of the CME (Simnett et al., 2002). In a survey of five years of scatter-free beam-like near-relativistic electron events we have shown that there is no evidence near 1 AU for escaping near-relativistic electrons as a constituent of the electron population that produce the type III radio bursts. It has been suggested that the propagation of a disturbance along the sun from the flaring region to the well connected region might be responsible for the delays observed in the near-relativistic electron injection (Krucker et al. 1999). However, we have shown that the angle between the flaring region based on the observed Hα longitude and the foot point of an Archimedean spiral connecting to 1 AU (based on the local solar wind speed at 1 AU) do not order the delays observed in the injection of the near-relativistic electron events. We have shown that there is a good relationship between beam-like near-relativistic electron events and SOHO/LASCO observed coronal transients (mainly traditional CMEs), that the height of the CME at the time of the electron injection is a few R_O, and that the delay in the injection of the electrons after the CME launch is inversely proportional to the speed of the CME. We therefore conclude that the delays are not due to a disturbance propagating along the disk of the Sun from the flaring region to a well connected Archimedean foot point, but are due to the upward propagation of the coronal transient and subsequent shock acceleration and injection onto open field lines.

ACKNOWLEDGMENTS

We thank our colleagues in the EPAM and LASCO consortia for their support and contribution to the analysis of the data presented here. We are grateful to Michael L. Kaiser of NASA/GSFC for his help in the detailed analysis of the WIND/WAVES decametric radio emission. The work performed at the Johns Hopkins University Applied Physics Laboratory has been supported by NASA under task 009 of contract NAS5-97271 and LWS grant NAG512479. Computing facilities at the University of Birmingham were supported by Starlink.

REFERENCES

Bougeret, J. –L., M. L. Kaiser, P. J. Kellogg, R. Manning, K. Goetz, S. J. Monson, N. Monge, L. Friel, C. A. Meetre, C. Perche, L. Sitruk, and S. Hoang, Waves: The Radio and Plasma Wave Investigation on the WIND Spacecraft, *Space Sci. Rev*., **71**, 231, 1995.

Cliver, E. W., S. W. Kahler, M. A. Shea, and D. F. Smart, Injection Onsets of ~2 GeV Protons, ~1 MeV Electrons, and ~100 keV Electrons in Solar Cosmic Ray Flares, ApJ, **260**, 362-370, September1, 1982.

Gold, R. E., S. M. Krimigis, S. E. Hawkins III, D. K. Haggerty, D. A. Lohr, E. Fiore, T. P. Armstrong, G. Holland, and L. J. Lanzerotti, Electron Proton and Alpha Monitor on the Advanced Composition Explorer Spacecraft, *Space Sci. Rev*., **86**, 385, 1998.

Haggerty, D. K., and E. C. Roelof, Impulsive near-relativistic solar electron events: Delayed injection with respect to solar electromagnetic emission, ApJ, November 10, 2002.

Haggerty, D. K., E. C. Roelof, and M. L. Kaiser, Relative Timing of Impulsive Solar Electron Injections and Solar Electromagnetic Emissions, in Planetary Radio Emissions V, eds. H. O. Rucker, M. L. Kaiser, and Y. Leblanc, Austrian Academy of Sciences, 437-444, 2001.

Kahler, S., Injection Profiles of Solar Energetic Particles as Functions of Coronal Mass Ejection Heights, ApJ, **428**, 837-742, June 20, 1994.

Krucker, S., D. E. Larson, R. P. Lin, and B. J. Tompson, On the Origin of Impulsive Electron Events Observed at 1 AU, ApJ, **519**, 864-875, July 10, 1999.

Simnett, G. M., E. C. Roelof, and D. K. Haggerty, The Acceleration and Release of Near-relativistic electrons by CMEs, ApJ, November 10, 2002.

Simnett, G. M., Relativistic Electron Events in Interplanetary Space, Space Science Reviews, **16**, 275-323, 1974.